Surface and Interior Strain Fields Measured by Multiple-embedded-grid Moiré and Strain Gages

by G. Cloud and S. Paleebut

ABSTRACT—Surface and interior strain fields in thick specimens of polycarbonate have been measured by an embedded-multiple-grid moiré method. Interior gratings are photographed through intervening gratings. Coherent optical processing of grating records creates moiré fringe patterns. A correction procedure was developed to eliminate moiré errors caused by strain-induced gradients of refractive index. This procedure utilizes the refraction distribution as obtained from observation of a grating from opposite sides of a specimen. No measurements other than the normal moiré observations are required in order to find actual strains. The correction technique should be useful in refining the results obtained when other optical methods are used in three-dimensional situations. The method is utilized to determine strains on the surfaces and at the mid- and quarter-planes of thick compact tension specimens. Results obtained, after correction, agree with measurements made with embedded strain gages. Maximum tensile strain occurs on the midplane. The findings are rationalized by consideration of thickness and proximity to the crack tip.

Introduction

For many years, mechanicians have sought to extend their theoretical, computational, and experimental techniques to obtain dependable information about three-dimensional fields. Increased use of advanced materials and augmented demands for energy- and material-efficient designs have intensified the quest for three-dimensional methods and results.

In this investigation, a multiple-embedded-grid moiré method was developed to study the strain on the surfaces, quarterplanes, and midplane of thick specimens made of polycarbonate.[1-4] The idea of using embedded moiré gratings for strain measurement on one interior plane has been utilized several times before,[5-8] although there has been disagreement about the need to correct for errors resulting from stress-induced changes in the refractive index. Here the method is extended to investigate multiple planes as well as the surface of the same specimen. The grids on the surface and in the interior were recorded for the unloaded condition and for various loaded states using high-resolution photographic techniques. The interior gratings were photographed through the out-of-focus intervening gratings. Moiré fringes were extracted using optical Fourier processing. The fringe data were digitized and strain maps generated by computer. A correction procedure to eliminate the errors caused by the material refraction effect was derived. The need for such a correction for errors caused by gradients of refractive index is not unique to embedded-grid moiré. The developed approach could be used to reduce errors when other optical methods, such as speckle, moiré interferometry, or holo-interferometry are used to measure strain or deformation in the interior of solids. It is also possible that the material-refraction coefficient used in the derivation of the correction equations might be useful in stress analysis.

This improved three-dimensional moiré technique was utilized to determine the strain fields in the interior and on the surfaces of thick compact tension specimens built up from layers of polycarbonate. Given the fact that the moiré correction procedure was new, unproven, and empirically based, the interior and surface strains were also measured by resistance strain gages.

Many researchers have measured surface stresses and strain states in the vicinity of a crack, primarily as a step towards obtaining stress-intensity factors,[9-12] although some have been interested in exploring the fundamental assumptions and limitations of fracture mechanics.[13-15] Crack-tip-opening displacements in the interior can be much different from the surface value, owing to crack retardation and closure phenomena.[16] A difference in the shape of the plastic zone for the surface and for the midplane of a cracked specimen has been observed.[17,18] The strain near a crack tip in PMMA has been mapped using

G. Cloud is Professor, Michigan State University, Materials Science and Mechanics Department, East Lansing, MI 48824. S. Paleebut is Group Captain, Royal Thai Air Force Academy, Don Muang, Bankok, Thailand 10220.

Paper presented at Vth International Congress on Experimental Mechanics, Montreal, Canada, 1984.

Original manuscript submitted: August 30, 1991. Final Manuscript received: May 15, 1992.

a speckle method,[19] with the result that no variation of the stress-intensity factor through the thickness was found. Three-dimensional photoelasticity has yielded considerable information about the stress state in thick cracked specimens (cf. Refs. 20-22).

Materials and Specimens

Multilayer compact-tension specimens of Merlon polycarbonate were used for this study. Mechanical properties are summarized in Table 1.[23] Two types of specimens were used. One type, shown in Fig. 1, had two-way gratings on the surface, quarterplanes, and midplane. The other type incorporated electrical-resistance strain gages (RSGs) on the corresponding surface and interior planes. Gage layout differed for the two strain-gage specimens. One of them is pictured in Fig. 2. The locations of the 19 RSGs used in this specimen are given in Table 2. The second gaged specimen was similar except that it incorporated 22 gages, some of which were mounted off the crack plane and some at the side of the specimen opposite the crack. Type EA-06-015DJ-120 gages from Micromeasurements Inc., Raleigh, NC were used in one specimen, and type EP-08-015CK-120 gages were installed in the second specimen. The moiré and strain-gage specimens had the same dimensions, and they were machined from specimen blocks, each made from four rectangular pieces of polycarbonate sheet of 9.53-mm thickness laminated together. The four pieces were fastened together with epoxy resin (Epon 828 and Diethylene tetramine 100:8 by wt).

Copper grids (two-way gratings) of 20 dot/mm were printed on some of the pieces using a stencil method.[24] A grid side on the first piece was bonded to a clear side on the second piece. Nickel mesh with 20 ℓ/mm and 0.2032-mm thickness was placed between the second and third pieces (midplane). Finally, translucent copper grids were vacuum-deposited on the surface planes. The strain-gage specimens were assembled in the same way except that the gratings were replaced by arrays of resistance strain gages having a gage length of 0.38 mm.

One of the moiré specimens had a fatigue precrack induced in order to make a very sharp crack tip. Owing to the difficulty in maintaining a straight crack front in the fatigue precrack, the rest of the specimens were tested with only a sharp V notch. Results from both cracked and notched specimens are given below, but they should not be compared with one another.

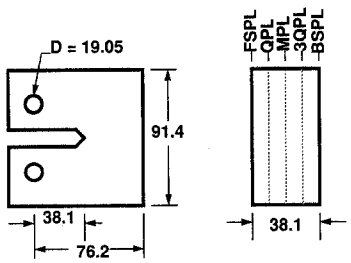

Fig. 1—Typical compact-tension specimen having surface and embedded grids

Experimental Procedure

Each compact-tension specimen was tested as shown schematically in Fig. 3. Loading was in a dead-weight load frame. For the experiments described in this paper, the nominal stress was 9.1 MPa. The camera was arranged to give a magnification of two. Each grid was imaged separately by focusing the camera on the grid plane to get maximum sharpness and contrast over the whole area near the crack tip. This high-resolution photography requires care, but it is not especially difficult.[1-4] Separate data plates were recorded by focusing on the front surface and

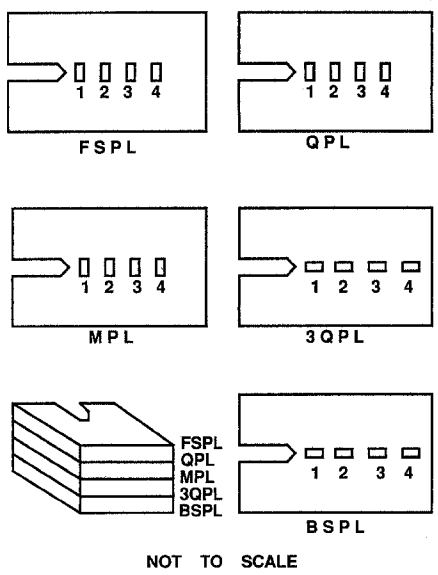

Fig. 2—Layout of surface and interior strain gages for gage specimen 1

TABLE 1—MECHANICAL PROPERTIES OF POLYCARBONATE (297 K)[23]

Upper Yield Strength (psi)	Lower Yield Strength (psi)	Tensile Strength (psi)	Modulus of Elasticity (psi)	Izod Impact (ft lb/in.)	Poisson's Ratio
8300	6600	9500	3.2×10^5	16.3	0.45-0.5

TABLE 2—POSITIONS OF STRAIN GAGES ON NOTCHED RSG SPECIMEN 1

Gage Position	Distance From Notch Tip or Preceding Gage, mm FSPL	QPL	MPL	3 QPL	BSPL
T-1	2.29	1.52	2.29	0.76	0.76
1-2	5.08	5.08	5.08	3.81	3.81
2-3	5.08	5.08	5.08	3.81	3.81
3-4	—	5.08	5.08	3.81	3.81

quarterplane in turn. The midplane and back surface were photographed after reversing the arrangement. Each interior grid was photographed through at least one intervening grid. Some loss of quality in the grid records was noted, but the results were adequate for successful optical processing. For each specimen, four plates were recorded at each specimen load state, including zero load.

Each photographic replica of a grid was treated by optical Fourier filtering to obtain moiré fringe patterns.[25] The light from a He-Ne laser was passed through a spatial filter which converted it to a moderately clean diverging beam. This beam was directed to a simple lens, whose output was parallel light. A moiré submaster grating (1-way lines) and one of the photoplates of a specimen grid were placed emulsion sides together in the optical path normal to the light beam. After passing through the photoplates, the beam, now containing diffraction components, was decollimated by a simple lens. At the focal plane, which is the transform plane of the field lens, there was placed a black paper screen containing a hole of approximately 2.4-mm diameter. This screen was retained in the filter mounting of a zoom lens mounted on a Nikon 35-mm camera. The hole in the filter mask was placed to coincide with the chosen ray group, a series of which appear as bright spots in the diffraction pattern. The image created in the camera by the light in the ray group contains interference fringes which are identical to moiré fringes which would be formed by simple mechanical superposition of gratings having spatial frequencies equal to those causing the diffraction in the optical processor. After final adjustment, each moiré fringe pattern was recorded on 35-mm film. The moiré fringe patterns were then enlarged and printed. Digitizing of the fringe patterns was performed on a Microdatatizer. The digitizing process was applied in turn to a moiré data photograph (specimen loaded) and a zero strain (specimen not loaded) baseline photograph. These two sets of digitized fringe data form a unit for computing and plotting of displacement and strain components. The strain values in both the x and y directions near the crack tip were calculated and plotted by using a computer program developed for moiré data-reduction.[1,3,25,26]

Interior Strain—Refraction Correction

The procedure outlined above was sufficient for determining surface strain fields. It soon became clear that the raw interior strain results required correction for local changes in refractive index of the polycarbonate. Because these changes are not uniform either through the thickness or in the lateral direction, they create an internal lens effect which changes the apparent pitch of the moiré gratings in the recorded grating image and so results in a false strain which is superimposed on the actual strain.

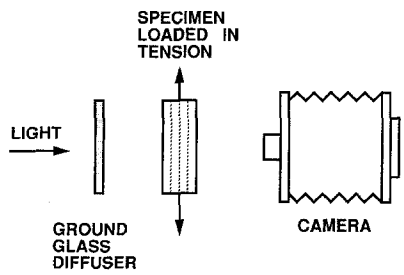

Fig. 3—Schematic of moiré testing setup

To illustrate the basis and magnitude of this refraction effect, moiré fringe patterns of the quarterplane of the specimen with a fatigue precrack are shown in Fig. 4. Typical apparent interior strains from a notched specimen, obtained directly from the data plates, are shown in Fig. 5. The strains near the crack tip along the crack line on the quarterplane and the midplane are compressive. These results are not in agreement with elastic solutions or with physical arguments.

Clearly, the unporrected data contain some type of large error. An obvious hypothesis is that the deformation and the deformation gradients caused gradients in the index of refraction sufficient to distort the moiré grid in the image photographs. That this effect is large enough to require correction has been noted before,[6] but other researchers have thought it negligible. In any case, no method for estimating or correcting the refraction errors has been devised. Another hypothesis is that 'dimpling' or other changes of surface curvature were created in this triaxial strain field. The curved surface would act as a lens and cause a distortion in the moiré image which would induce error in the strain results. Visual examination, calculations, and an experiment with an immersion medium demonstrated that any errors from this lens effect were small enough to ignore completely.

The refraction effect was studied by using specimens one-quarter and one-half the thickness of the test specimen and having copper gratings deposited on only one side. These two specimens were photographed from both sides. The apparent strain differences between the two replicas from both specimens were plotted as a function of specimen thickness with the result shown in Fig. 6. The relation between strain difference and specimen thickness is found to be represented accurately by

$$y = a x^2 \tag{1}$$

where y is apparent strain difference, a is a coefficient depending on material, and x is material thickness through which the grating is viewed. This empirical relationship served as a guide (only) in creating a procedure for reducing or eliminating refraction-induced errors in the strain measured with interior gratings.

Now, actual strains on a given quarterplane in the interior of a specimen that were obtained from photographs of the specimen grid through one-quarter thickness and through three-quarter thickness must be identical. That the results are not the same is shown in Fig. 7. Forcing the two results to be identical yields information which fixes the coefficient in eq (1) for the interior measurements. The development of this idea for estimating strain corrections is as follows:

$$\begin{aligned} \epsilon_{m1} &= \epsilon_{R1} + \Delta\epsilon_1 \\ \epsilon_{m3} &= \epsilon_{R3} + \Delta\epsilon_3 \end{aligned} \tag{2}$$

where ϵ_{m1} and ϵ_{m3} are strains measured on a given quarterplane by taking photographs of the grid through one-quarter thickness and through three-quarter thickness. ϵ_{R1} and ϵ_{R3} are the real strains on this particular quarterplane, so, $\epsilon_{R1} = \epsilon_{R3}$. $\Delta\epsilon_1$ and $\Delta\epsilon_3$ are strain errors induced by taking the photograph of the inner grid through a one-quarter thickness and through a three-quarter thickness of material.

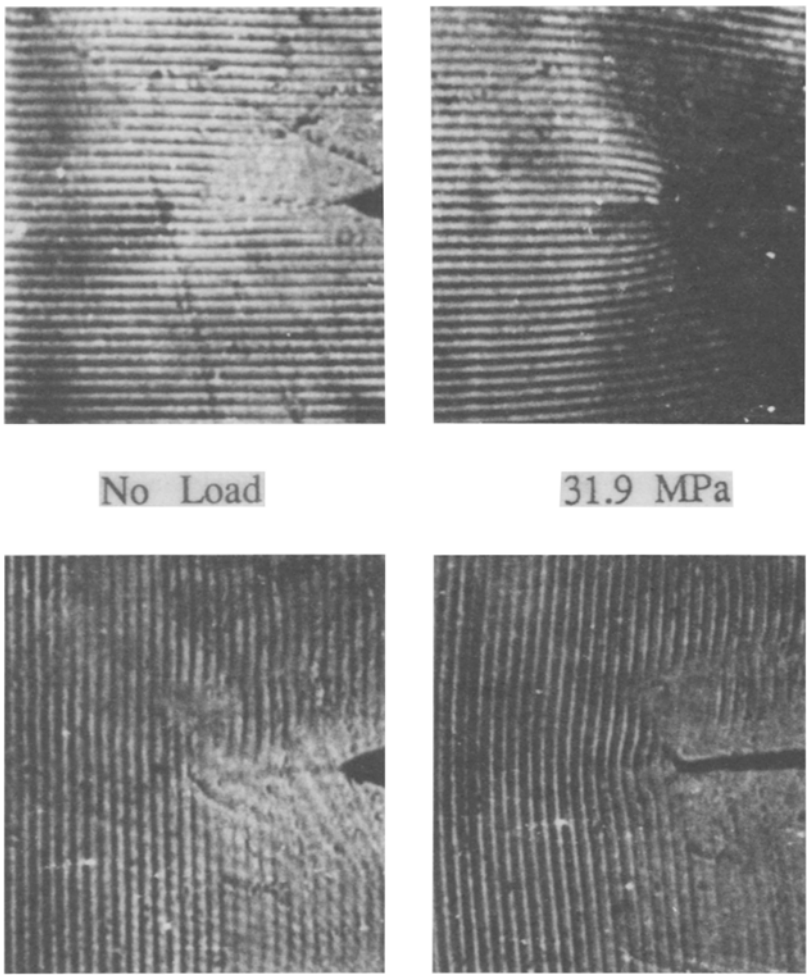

Fig. 4—Typical moiré fringe pattern for quarter plane of fatigue crack specimen for submaster grating of 20 lines per mm: (a) parallel to crack line; (b) perpendicular to crack line

On the basis of empirical observations leading to eq (1), it is reasonable to write

$$\Delta\epsilon = \delta \left(\frac{d}{B}\right)^2 \tag{3}$$

where

δ = empirical refraction coefficient
d = distance from near surface to observed specimen grating
B = total specimen thickness.

Combining eqs (2) and (3) gives

$$\epsilon_{m1} = \epsilon_{R1} + \delta(1/4)^2$$
$$\epsilon_{m1} = \epsilon_{R3} + \delta(3/4)^2 \tag{4}$$

Solving for the material coefficient gives

$$\delta = 2(\epsilon_{m3} - \epsilon_{m1}) \tag{5}$$

The material refraction coefficient is of little interest in the analysis of strain, although it would likely be important in investigations of optical properties of materials. It can be eliminated by combining the preceding equations. Substituting and solving for the actual strain yields the

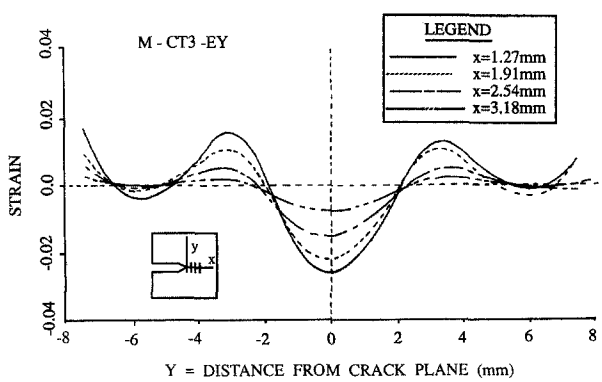

Fig. 5—Apparent strain, before correction for refraction effects, on midplane of notched specimen

following:

real strain on the quarterplane

$$(\epsilon_{R1}) = (9\epsilon_{m1} - \epsilon_{m3})/8 \quad (6)$$

real strain on the midplane

$$(\epsilon_{R2}) = \epsilon_{m2} - (\epsilon_{m3} - \epsilon_{m1})/2 \quad (7)$$

These equations show that the actual strain on two interior planes can be estimated from three moiré observations of the same planes, even though the moiré data are contaminated by errors resulting from strain-induced gradients in refractive index.

Experimental Results

The data obtained from three-dimensional studies of several different specimens are profuse and complex. There is no possibility of presenting here more than a few typical examples of results and the major conclusions and comments. Subtle aspects of the study must be ignored. Complete data and discussion in depth may be found in the relevant report.[1]

It is useful to divide the following discussion into two parts, one related to surface strain data and the other concerning interior results. In all the discussion, the crack is visualized as lying in a horizontal plane, so 'vertical' strain means the component perpendicular to the crack plane, and so on.

Surface and interior strain-gage results from one of the gaged specimens are shown in Table 3. These data are utilized for comparisons at various points in the following sections. During strain-gage testing, steps were taken to minimize effects of heating in the embedded gages.

TABLE 3—STRAIN RESULTS FROM NOTCHED RSG SPECIMEN 1

Gage No.	Vertical Strain FPL	QPL	MPL	Horizontal Strain 3 QPL	BPL
1.	0.00091	0.00210	0.00197	0.00129	0.00092
2.	0.00020	0.00053	0.00065	0.00129	0.00111
3.	−0.00024	0.00014	0.00011	0.00096	0.00082
4.	—	−0.00028	—	0.00065	0.00065

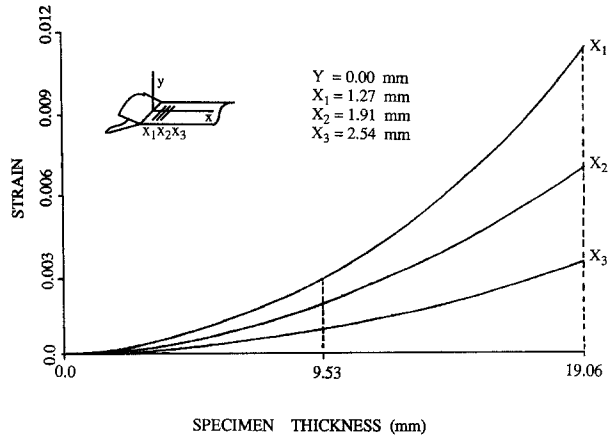

Fig. 6—Plot of difference in apparent strain taken from opposite sides of demonstration specimen for various axes in the crack plane

Surface Strain

Consider first the measured surface strain fields. Figure 8 shows typical moiré fringe patterns for undeformed and deformed states corresponding to both vertical and horizontal surface gratings of the specimen with a fatigue precrack. Typical vertical strain on the surface as a function of vertical distance from the crack line for axes at various 'small' distances from the crack tip are shown in Fig. 9. Surface vertical and horizontal strains as obtained with moiré and with strain gages versus distance along the

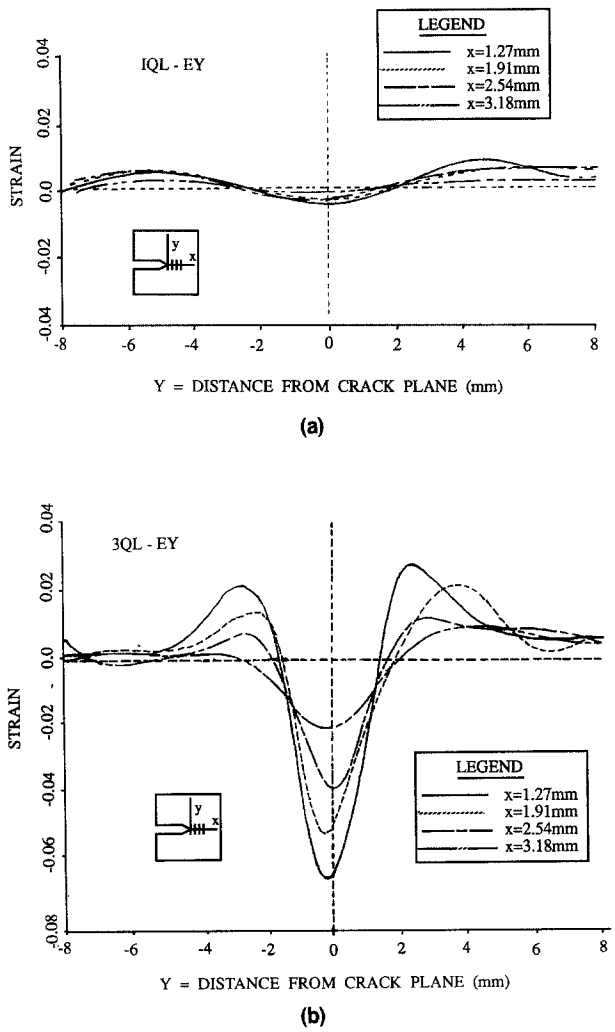

Fig. 7—Apparent vertical strain in quarter plane of crack specimen obtained by grid photography through: (a) one-quarter side of specimen; (b) three-quarter side of specimen

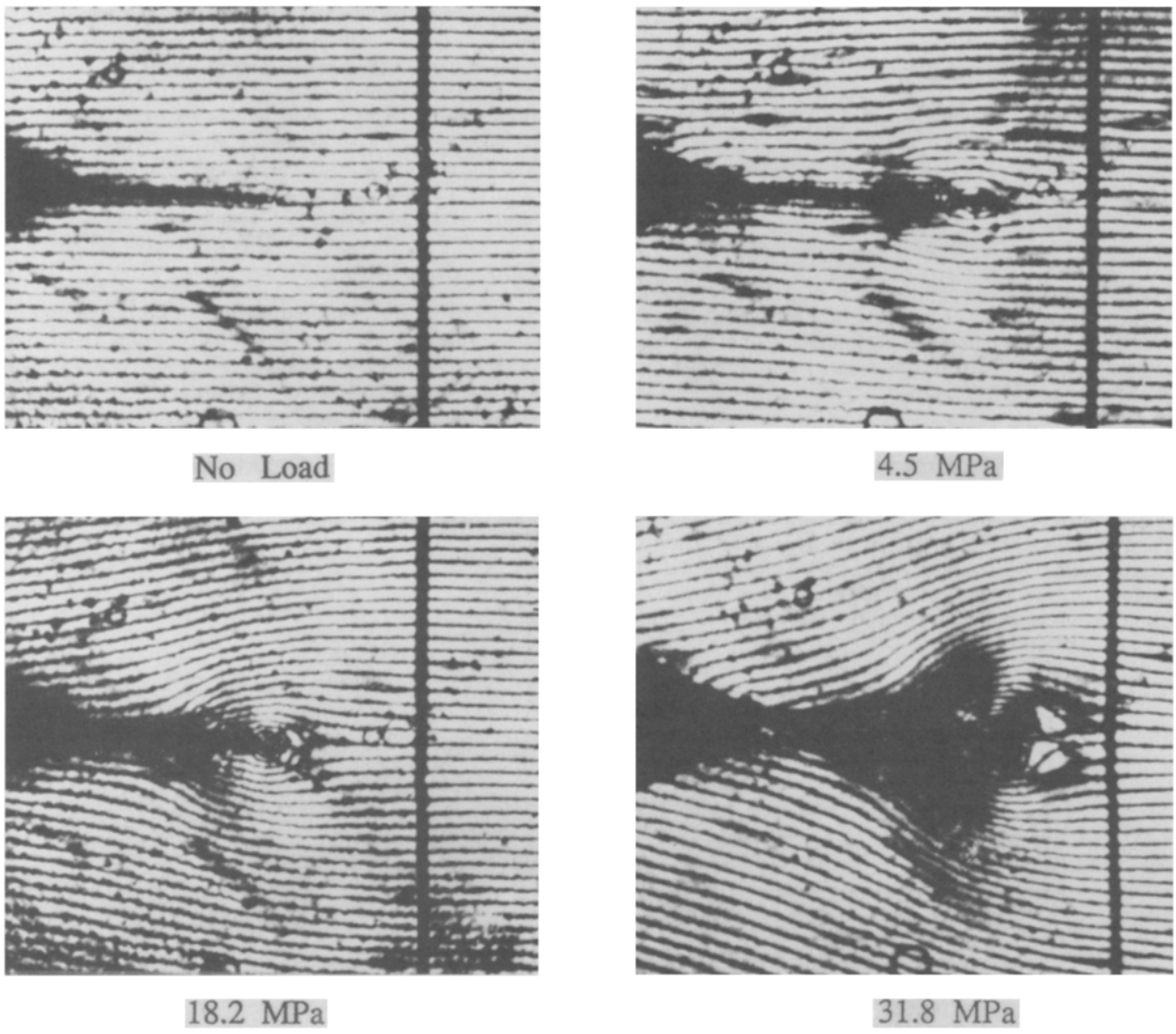

Fig. 8—Typical moiré fringe patterns from surface of specimen with fatigue crack

crack line for cracked and notched specimens are summarized in Figs. 10(a) and 10 (b) (note scaling differences). These results show that maximum surface tensile strain in the vertical direction occurs near the crack tip. Vertical strain is tensile only within a small distance near the crack tip; it changes to compressive strain further out. The maximum compressive strain in the vertical direction occurs at the surface furthest from the crack tip. It is worth recalling that, in these compact tension specimens, both tensile and bending stresses are acting. For a specimen in which crack length is one half of specimen width, $a = w/2$, the effect of loading in bending is nine times that of tension loading.[27]

Interior Strain

The apparent strains in the interior of the notched specimen that were obtained directly from the gratings, as shown in Fig. 5, were corrected by using eqs (6) and (7) and compared with the strain-gage results. Figures 11 and 12 are the plots of corrected strain values along the crack line for each interior and surface plane studied. Results from the specimens with strain gages are also shown on these plots. The strain gage and the moiré results are in excellent agreement.

The moiré results permitted construction of full-field strain contours for each plane studied. Space is not adequate to present these maps here. They are useful for visualizing the three-dimensional nature of the strain field. A sample plot showing contours of equal vertical strain on the midplane is reproduced in Fig. 13.

Discussion

This study is focused primarily on the experimental approach and the demonstration of its application to a problem in fracture mechanics. Space limitations preclude a complete quantitative analysis of the fracture data. Some general observations about these results and their relationships with the work of other investigators are

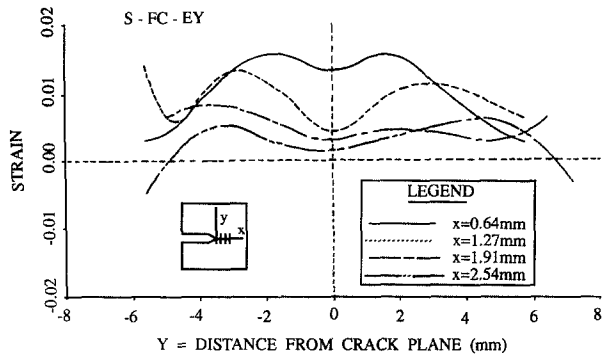

Fig. 9—Surface strain ϵ_y perpendicular to crack line for axes at various distances from crack tip in fatigue crack specimen

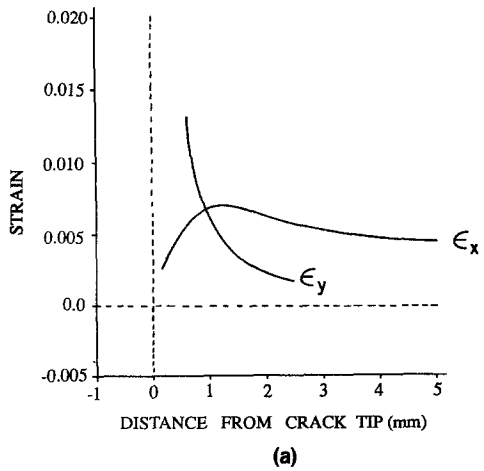

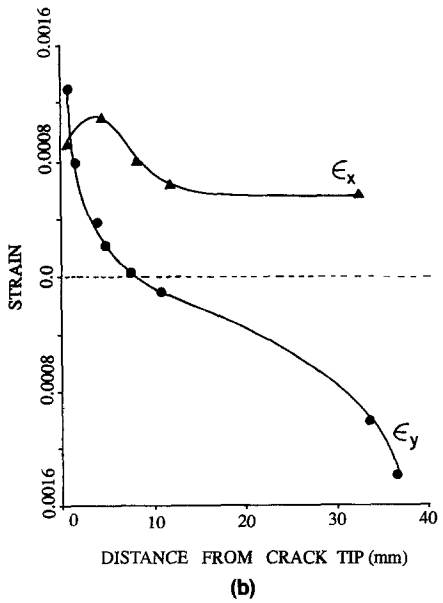

Fig. 10—Summary plot of surface strains ϵ_x and ϵ_y along the crack line of specimen obtained: (a) by moiré method for fatigue crack; (b) by strain gages for notch

offered below, as they are useful and instructive. More detailed analyses derived from the methodology and results reported above appear elsewhere.[28-31]

From the elementary theory of linear-elastic fracture mechanics (LEFM) and the stress–strain relations, the

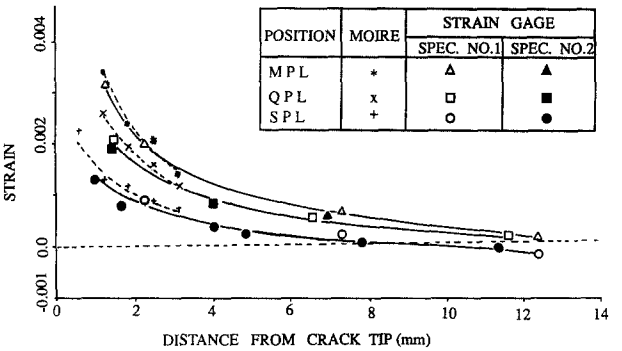

Fig. 11—Summary plot of strain perpendicular to crack plane from corrected moiré data and strain-gage data for notched specimen

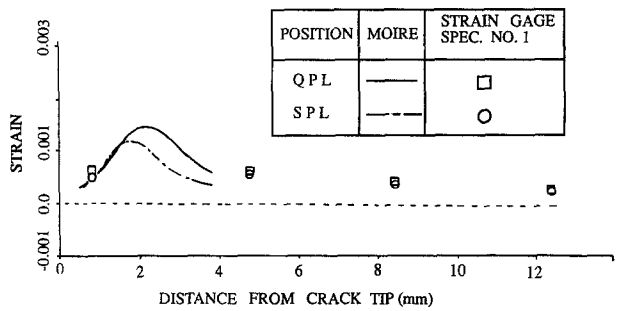

Fig. 12—Summary plot of strain parallel to crack plane from corrected moiré data and strain-gage data for notched specimen

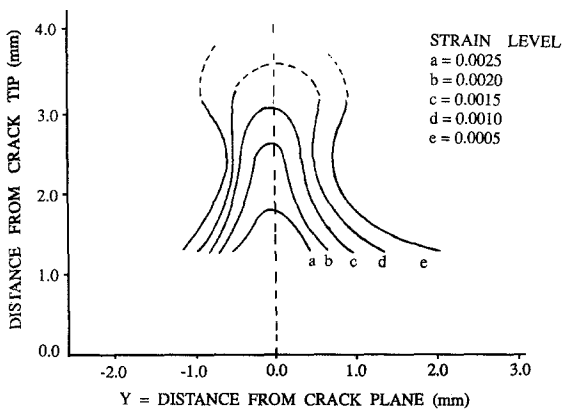

Fig. 13—Contours of constant ϵ_y near the crack tip in the midplane for notched specimen

strain on the surface is predicted to be larger than on the midplane. The results of this investigation disagree with the theory of LEFM in that, in almost every case, higher strain was measured in the interior near the crack tip. The stress-intensity factor along a straight crack in the standard CT specimen is maximum at the center plane and minimum at the surface. At the time this research was performed and the results for the interior planes first presented,[1,2] they were rejected by some in the fracture-mechanics community. Greater understanding of the stress field in thick specimens has led to acceptance.

These findings do agree with the results obtained with three-dimensional FEM programs.[32-35] Also, a photoelastic study[36] showed that K_I in the center slice was five to ten-percent higher than average through the thickness. The radius of curvature in notched bent steel specimens was found to be greater at specimen midsection than at the outside.[37] The crack-opening displacements of bent steel specimens have been measured by a rubber infiltration technique and found to be greater in the interior.[38]

It is worth noting that the surface strain distributions seem to match the surface stress distributions determined through photoelasticity by various investigators including Gerberich,[39] Kobayashi, Engstorn, and Simon[40] and Liu and Ke.[41] The interior strain distributions, of which a sample is shown in Fig. 13, are found to differ significantly from the surface field.

Consider further the comparisons of experiment and linear theory. An elastic solution[42] predicts that, *at the crack tip* ($r \approx 0$), $\sigma_x = 0$ and σ_y on the midplane is larger than σ_y on the surface. This prediction agrees with an experimental result.[12] It is possible, then, to have σ_y on the midplane larger than σ_y on the surface plane *right at* the crack tip.

For $r > 0$, that is, inside a small but finite region near the crack tip, it is suggested that[43,44]

$$\sigma_y(r,0) = \frac{K_I}{\sqrt{2\pi r}} + 0(r^{1/2})$$
$$\sigma_x(r,0) = \frac{K_I}{\sqrt{2\pi r}} - \sigma_{ox} + 0(r^{1/2}) \quad (8)$$

The added term, σ_{ox}, corresponds to local stress acting parallel to the center crack at its tip. $0(r^{1/2})$ are higher-order terms which customarily are assumed to be negligible.

If eqs (8) are substituted into the stress-strain relationships for plane stress and plane strain, one obtains

$$\epsilon_y(r,0) = \frac{1}{E}\left[(1-\nu)\frac{K_I}{\sqrt{2\pi r}} + \nu\sigma_{ox}\right] \text{ for plane stress}$$
$$\epsilon_y(r,0) = \frac{1}{E}\left[(1-\nu-2\nu^2)\left(\frac{K_I}{\sqrt{2\pi r}}\right) + \nu(1+\nu)\sigma_{ox}\right]$$
$$\text{for plane strain} \quad (9)$$

For the material used in this study, $\nu = 0.45$. For the thick specimens used, it is assumed that the surface plane is in plane stress and the midplane is in plane strain. If K_I on the midplane is larger than on the surface plane, and if σ_{ox} is a large value, then it is possible to have vertical strain on the midplane larger than on the surface plane for $r > 0$. It follows that the vertical strain along the crack line on the midplane must be larger than its values on the surface plane. Such a conclusion is supported by the results obtained in this study. The σ_{ox} is an important factor for the conditions of this investigation.

Consideration of energy dissipation and plastic zone sizes in the interfacial cement and in the polycarbonate lamina offer potentially valuable insight into the behavior of these multilayer specimens. Such arguments are somewhat speculative and do not fall within the scope of this report.

Summary and Conclusions

Embedded-grid Technique

The multiple embedded-grid moiré method is useful for studying three-dimensional problems. The technique is simple, and it requires no measurements other than the usual moiré grid records. Grating records obtained from the interior, even though photographed through intervening gratings, are good enough to form useful moiré fringe patterns when processed with an elementary optical Fourier analyzer.

Stress-induced gradients in refractive index cause distortions of the grid records, and so create serious errors in the moiré data for interior planes. A correction procedure was developed to eliminate moiré errors caused by refraction. This procedure utilizes the refraction distribution as obtained from observation of a grating from opposite sides of the specimen. That is, there is no need for extra observations in order to establish the correction for refraction error.

The results that were obtained from the moiré technique after correction were compared with measurements made with embedded strain gages. The agreement was excellent.

There are some obvious shortcomings to the embedded-grating approach. Any three-dimensional analysis is complex, and this method is no exception. The technique also is not actually three-dimensional, as it gives strains only in the planes of the gratings. Further, the demonstration described here is for a strain field which is more or less symmetrical with respect to the central plane of the specimen. Finally, the magnitude of the refraction correction relative to the actual strain is cause for concern.

The method utilizes an empirically based estimate of the profile of the refraction error, with the size of the correction based on measurements in discrete planes. Certainly, there is need for further investigation of the characteristics of the refraction effect and refinement of methods for its removal.

While there is no need for strain-field analysis to actually measure the refraction coefficient, direct observation of the refraction effect is possible using the ideas presented above. Such a procedure could be correlated with the methods of caustics, strain gradients and isodynes (cf. Refs. 45 and 46) to augment our limited insight into the three-dimensional nature of complex strain fields.

The embedded-grating approach could be used to measure crack-tip-opening displacement in the interior as well as on the surface.[1]

Errors in strain measurement caused by strain-induced gradients of refractive index are not unique to embedded-grid moiré analysis. The correction procedure derived and demonstrated above is also not restricted to moiré investigations. The approach should serve well when other optical techniques, including grid methods, moiré interferometry, holointerferometry, speckle methods, and shearography, are used in applications where the light must traverse material containing stress states which are significantly three dimensional.

Crack Mechanics

Tensile strain, ϵ_y, occurs only in a small area near the crack tip in the thick specimens of polycarbonate. ϵ_y is a maximum on the midplane, and it causes crack initiation to start at midplane. Near the crack tip, ϵ_y, is much greater than ϵ_x on any plane though the specimen thickness. In the interior, the line of maximum ϵ_y starts at the crack tip and lies in the crack plane. On the surface, the maximum ϵ_y occurs along lines radiating from the crack tip.

The strain distributions observed agree in general form with the findings of other experimenters. At first glance, the results seem incompatible with elementary fracture mechanics. Consideration of effects of thickness, plastic zone, and proximity to crack lead to the conclusion that theory and experiment agree provided proper attention is given to the induced local normal stress acting parallel to the crack front.

Acknowledgment

This research was begun with support by the National Science Foundation under Grant No. ENG2802530. The work was continued under a grant from the Research Excellence Fund of the State of Michigan. The authors are wholly grateful to Mr. Subrato Dhar for several valuable contributions to this work.

References

1. Paleebut, S., An Experimental Study of Three-Dimensional Strain Around Coldworked Holes and In Thick Compact Tension Specimens, PhD Thesis, Michigan State Univ., E. Lansing, Michigan 48823 (1982).

2. Cloud, G.L. and Paleebut, S., "Surface and Interior Strain in Thick Crack Specimens Measured by Multiple Embedded Grid Moiré and Strain Gages," Proc. 5th Int. Cong. on Exp. Mech., SEM (June 1984).

3. Cloud, G. and Paleebut, S., "Three-Dimensional Nature of Strain Field Near Coldworked Holes," Tech. Rep. AFWAL-TR-80-4204, Air Force Materials Lab., Wright-Patterson AFB Ohio 45433 (1980).

4. Cloud, G.L. and Paleebut, S., "Surface and Internal Strain Fields Near Coldworked Holes Obtained by a Multiple Embedded-Grid Moiré Method," Eng. Fract. Mech., **19** *(2), 375-381 (1984).*

5. Durelli, A.J. and Daniel, I.M., "A Nondestructive Three-Dimensional Strain Analysis Method," J. Appl. Mech., **28** *(3), 83-86 (May 1961).*

6. Kerber, R.C. and Whittier, J.S., "Moiré Interferometry with Embedded Grids-Effect of Optical Refraction," EXPERIMENTAL MECHANICS, **9** *(5), 203-209 (May 1969).*

7. Bremond, C. and Durelli, A.J., "Experimental Analysis of Displacements and Shears at Surfaces of Contact," EXPERIMENTAL MECHANICS, **21** *(3), 105-110 (1981).*

8. Sciammarella, C.A. and Chiang, F.P., "The Moiré Method Applied to Three-Dimensional Elastic Problem," EXPERIMENTAL MECHANICS, **4** *(11), 313-319 (Nov. 1964).*

9. Evans, W.T. and Luxmoore, A., "Measurement of In-plane Displacement Around Crack Tips by a Laser Speckle Method," Eng. Fract. Mech., **6**, *735-743 (1974).*

10. Somer, E., "An Optical Method for Determining the Crack Tip Stress Intensity Factor," Eng. Fract. Mech., **1**, *705-718 (1970).*

11. Closeley, P.B., Mostovey, S. and Eipling, E.J., "An Optical Method for Experimental Stress Analysis of Crack Structures," Eng. Fract. Mech., **3**, *421-433 (1971).*

12. Marloff, R.H., Levan, M.J., Ringler, T.N. and Johnson, R.L., "Photoelastic Determination of Stress Intensity Factors," EXPERIMENTAL MECHANICS, **11** *(12), 529-539 (Dec. 1971).*

13. Stormont, C.W., Gonzalez, H., Jr. and Brinson, H.F., "The Ductile Fracture of Anisotropic Materials," EXPERIMENTAL MECHANICS, **12** *(12), 557-563 (Dec. 1972).*

14. Villarreal, G., Sih, G.C. and Hartranft, R.J., "Photoelastic Investigation of a Thick Plate with a Transverse Crack," J. Appl. Mech., **42** *(1), 9 (March 1975).*

15. Mills, N.J., "Dugdale Yielded Zones in Cracked Sheets of Glassy Polymers," Eng. Fract. Mech., **6**, *537-549 (1974).*

16. Pitoniak, F.J., Grandt, A.F., Montulli, L.T. and Packman, P.E., "Fatigue Crack Retardation and Closure in Polymethylmethacrylate," Eng. Fract. Mech., **6**, *663-670 (1974).*

17. Hahn, G.T. and Rosenfield, A.R., "Sources of Fracture Toughness; The Relation Between K_{IC} and the Ordinary Tensile Properties of Metals," ASTM-STP 432, 5-32 (1968).

18. Underwood, J.H. and Kendall, D.P., "Measurement of Microscopic Plastic-Strain Distributions in the Region of a Crack Tip," EXPERIMENTAL MECHANICS, **9** *(7), 296-304 (July 1969).*

19. Barker, D.B. and Fourney, M.E., "Three-Dimensional Interferometric Investigation of the Stress Intensity Factor Along a Crack Front," EXPERIMENTAL MECHANICS, **17** *(7), 241-247 (July 1977).*

20. Smith, C.W., "Use of Three Dimensional Photoelasticity and Progress in Related Areas," Experimental Techniques in Fracture Mechanics, ed. A.S. Kobayashi, Iowa State University Press, Ames, IA, **2**, *3-58 (1975).*

21. Smith, C.W., Post, D., Hiatt, G. and Nicoletto, G., "Displacement Measurement around Cracks in Three-Dimensional Problems by a Hybrid Experimental Technique," EXPERIMENTAL MECHANICS, **20** *(4), 15-20 (1983).*

22. Smith, C.W. and Epstein, J.S., "Measurement of Three-Dimensional Effects in Cracked Bodies," Proc. 5th Int. Cong. on Exp. Mech., SEM (June 1984).

23. An Engineering Handbook on Merlon Polycarbonate, Mobay Chemical Company, Pittsburgh, PA.

24. Luxmoore, A.R. and Hermann, R., "The Rapid Deposition of Moiré Grids," EXPERIMENTAL MECHANICS, **11** *(8), 375-377 (Aug. 1971).*

25. Cloud, G.L., "Simple Optical Processing of Moiré Grating Photographs," EXPERIMENTAL MECHANICS, **20** *(8), 265-272 (Aug. 1980).*

26. Cloud, G.L., "Residual Surface Strain Distribution Near Holes Coldworked to Various Degrees," Tech. Rep. AFML-TR-78-153, Air Force Materials Lab., Wright Aeronautical Laboratories, Ohio (Nov. 1978).

27. Tada, H., Paris, P. and Irwin, G., The Stress Analysis of Crack Handbook, Del Research Corporation, Hellertown, PA.

28. Dhar, S., Cloud, G.L. and Paleebut, S., "Measurement of Three-Dimensional Mode-1 Stress Intensity Factor Using Multiple Embedded Grid Moiré Technique," Theor. and Appl. Fract. Mech., **12** *(2), 141-147 (Dec. 1989).*

29. Cloud, G. and Dhar, S., "Energy Density Approach for Calculation of Inelastic Strain and Stress at the Crack Tip in Compact Tension Specimens of Polycarbonate," Proc. 1990 Spring Conf. on Exp. Mech., SEM (June 1990).

30. Dhar, S. and Cloud, G., "Application of Strain Energy Density to Calculation of Inelastic Strain at the Crack Tip," Proc. "Fatigue 90"; 4th Int. Conf. on Fatigue and Fatigue Threshold, Honolulu, HI (July 1990).

31. Dhar, S. and Cloud, G., "Energy Density Approach for Calculation of Inelastic Three-Dimensional Strain and Stress at the Crack Tip in Compact Tension Specimens of Polycarbonate," Int. J. Fract., **52**, *229-248 (1992).*

32. Tracey, D.M., "Three-Dimensional Elastic Crack Analysis," Nucl. Eng. and Design, **26** *(2), 282-290 (1974).*

33. Reynen, J., "On the Use of Finite Elements in Fracture Analysis of Pressure Vessel Components," Trans. ASME J. Press. Vess. Tech., 75-PVP-20, 1-9 (1975).

34. Raju, I.S. and Newman, J.C., "Three-Dimensional Finite Element Analysis of Finite Thickness Fracture Specimens," NASA Tech. Note, NASA TN D-8414 (1977).

35. Neale, B.K., "The Stress Intensity Factors Associated with Curved Crack Fronts in a Compact Tension Specimen," Numerical Methods in Fracture Mechanics, ed. A.R. Luxmoore and D.R.J. Owen, Proc. First Int. Conf., University College Swansea, Swansea SA2 8PP, West Glamorgan, UK (Jan. 1978).

36. Schroedl, M.A. and Smith, C.W., "Influence of Three-Dimensional Effect on the Stress Intensity Factors for Compact Tension Specimen," Fract. Anal. ASTM STP 560, 64-80 (1974).

37. Lequear, H.A. and Lubahn, J.D., "Root Conditions in a V-Notch Charpy Impact Specimen," Weld. Res. Suppl., **33**, *585-S-588-S (1954).*

38. Robinson, J.N. and Tetelman, A.S., "The Relationship Between Crack Tip Opening Displacement, Local Strain and Specimen Geometry," Int. J. Fract., **11**, *453-468 (1975).*

39. Gerberich, W.W., "Plastic Strains and Energy Density in Crack Plates, Part 1 - Experimental Technique and Results," EXPERIMENTAL MECHANICS, **4** *(11), 335-344 (Nov. 1964).*

40. Kobayashi, A.S., Engstorn, E.L. and Simon, B.R., "Crack Opening Displacements and Normal Strains in Centrally Notched Plates," EXPERIMENTAL MECHANICS, **9** *(4), 163-170 (1969).*

41. Liu, H.W. and Ke, J.S., "The Measurement of Fracture Toughness of Ductile Materials," Eng. Fract. Mech., **5**, *187-202 (1973).*

42. Boyd, G.M., "From Griffith to COD and Beyond," Eng. Fract. Mech., **4** *(3), 459-482 (1972).*

43. Irwin, G.R., "Analysis of Stresses and Strains Near the End of a Crack Traversing a Plate," J. Appl. Mech., **24**, *361-364 (Sept. 1957).*

44. Cotterell, B. and Rice, J.R., "Slightly Curved or Kinked Cracks," Int. J. Fract., **16**, *155-169 (1980).*

45. Pindera, J.T. and Hecker, F.W., "Basic Theory and Experimental Techniques of the Strain-Gradient Method," EXPERIMENTAL MECHANICS, **27** *(3), 314-327 (Sept. 1987).*

46. Pindera, J.T., Krasnowski, B.R. and Pindera, M.J., "Theory of Elastic and Photoelastic Isodynes. Samples of Application in Composite Structures," EXPERIMENTAL MECHANICS, **25** *(3), 272-281 (Sept. 1985).*